INTERNATIONAL DENTAL JOURNAL 000 (2023) 1–11

Scientific Research Report

Loricrin and Cytokeratin Disorganisation in Severe Forms of Periodontitis

Raisa Queiroz Catunda [a], *Karen Ka-yan Ho* [a], *Srushti Patel* [a], *Christopher Bryant Roy* [a], *Maria Alexiou* [a], *Liran Levin* [a], *Benjamin J. Ulrich* [b], *Mark H. Kaplan* [c], *Maria Febbraio* [a*]

[a] *Department of Dentistry, College of Health Sciences, University of Alberta, Edmonton, Alberta, Canada*
[b] *Northwestern University, Chicago, Illinois, USA*
[c] *Department of Microbiology & Immunology, School of Medicine, Indiana University, Indianapolis, Indiana, USA*

ARTICLE INFO

Article history:
Received 30 December 2022
Received in revised form
5 May 2023
Accepted 22 May 2023
Available online xxx

Key words:
Loricrin
Periodontal disease
Epithelial barrier
Stat6VT

ABSTRACT

Objective: The aim of this research was to investigate the role of the cornified epithelium, the outermost layer of the oral mucosa, engineered to prevent water loss and microorganism invasion, in severe forms of periodontitis (stage III or IV, grade C).

Methods: Porphyromonas gingivalis, a major periodontal disease pathogen, can affect cornified epithelial protein expression through chronic activation of signal transducer and activator of transcription 6 (Stat6). We used a mouse model, Stat6VT, that mimics this to determine the effects of barrier defect on *P gingivalis*–induced inflammation, bone loss, and cornified epithelial protein expression, and compared histologic and immunohistologic findings with tissues obtained from human controls and patients with stage III and IV, grade C disease. Alveolar bone loss in mice was assessed using micro-computerised tomography, and soft tissue morphology was qualitatively and semi-quantitatively assessed by histologic examination for several proteins, including loricrin, filaggrin, cytokeratin 1, cytokeratin 14, a proliferation marker, a pan-leukocyte marker, as well as morphologic signs of inflammation. Relative cytokine levels were measured in mouse plasma by cytokine array.

Results: In the tissues from patients with periodontal disease, there were greater signs of inflammation (rete pegs, clear cells, inflammatory infiltrates) and a decrease and broadening of expression of loricrin and cytokeratin 1. Cytokeratin 14 expression was also broader and decreased in stage IV. *P gingivalis*–infected Stat6VT mice showed greater alveolar bone loss in 9 out of 16 examined sites, and similar patterns of disruption to human patients in expression of loricrin and cytokeratins 1 and 14. There were also increased numbers of leukocytes, decreased proliferation, and greater signs of inflammation compared with *P gingivalis*–infected control mice.

Conclusions: Our study provides evidence that changes in epithelial organisation can exacerbate the effects of *P gingivalis* infection, with similarities to the most severe forms of human periodontitis.

Introduction

The cornified epithelium (CE), which is the outermost layer of the skin, has a similar representation in the oral cavity and is known as keratinised epithelium.[1,2] It acts as a physical, mechanical, and immunologic barrier against external aggressors and water loss.[3,4] The CE is created through a tightly regulated differentiation process to yield cell bodies

* *Corresponding author*. Department of Dentistry, College of Health Sciences, University of Alberta, 7020M, Katz, 11361-87th Avenue, Edmonton, Alberta, Canada, T6G 2E1.
E-mail address: febbraio@ualberta.ca (M. Febbraio).
Raisa Queiroz Catunda: http://orcid.org/0000-0001-5589-402X
Karen Ka-yan Ho: http://orcid.org/0000-0002-6668-9598
Srushti Patel: http://orcid.org/0000-0001-7761-0200
Liran Levin: http://orcid.org/0000-0002-8123-7936
Benjamin J. Ulrich: http://orcid.org/0000-0002-2729-1798
Mark H. Kaplan: http://orcid.org/0000-0002-2923-8245
https://doi.org/10.1016/j.identj.2023.05.004

containing keratin, intermediate filaments and lipids embedded in a scaffold under the cell membrane, formed from proteins from the granular layer (eg, loricrin, involucrin, filaggrin).[1,2,4] Barrier dysfunction plays a significant role in the pathogenesis of diseases such as atopic dermatitis (AD), psoriasis, loricrin keratoderma and, potentially, periodontitis.[5]

The different proteins of the CE are fundamental to barrier integrity. Loricrin, an insoluble polypeptide, composes approximately 70% to 80% of the cornified envelope.[6] It is intra-crosslinked and inter-crosslinked to involucrin by transglutaminases. Filaggrin, like loricrin, is a structural protein, responsible for the aggregation and correct incorporation of keratin filaments in cornified cells.[1,2] Cytokeratins (CK) constitute the structural foundation of epithelial cells. CK1 expression normally increases during cell turnover and healing processes; downregulation may be considered a marker of chronic epithelial stress.[7] CK 14 is expressed in proliferating keratinocytes; those that enter the differentiation pathway lose expression. Inappropriate expression of CK14 is often observed in chronic wounds.[8] Given the functions of these proteins, we reasoned that alterations could profoundly affect the healing abilities of the oral epithelium and contribute to accelerated periodontal disease progression.

Barrier dysfunction in AD has been shown to mechanistically involve decreased CE protein expression due to increased levels of T-helper cell 2 (Th2) cytokines, including interleukin (IL)-4.[9-13] IL-4 signaling in keratinocytes is mediated by the Janus kinase (Jak) 2-signal transducer and activator of transcription (Stat) 6 pathway (Figure 1a).[13-15] When there is chronic IL-4 signaling/Stat6 activation, a shared cofactor, p300/Creb-binding protein (CBP) is sequestered and loricrin and filaggrin gene expression are downregulated (Figure 1b).[13,14]

Whilst a dysfunctional epithelial barrier has been vastly studied in skin, there is reason to suspect that it may also affect the oral cavity.[2,13,16-25] Studies have shown that *Porphyromonas gingivalis* (Pg), an important periodontal disease (PD) pathogen, can affect changes in barrier function and CE protein expression by direct and indirect mechanisms.[18-24] Recently, PD classification has changed to reflect a spectrum disorder, and formerly aggressive periodontitis is now designated as stage III or IV, grade C.[26] For simplicity, we refer to these forms as severe periodontitis (SvP) IIIC and IVC. Like AD, SvP is characterised by a Th2 response, and studies have shown that in SvP there is profound downregulation of the CE genes loricrin and filaggrin.[27-33] However, these studies did not address protein expression or disease manifestation.

An extensively used mouse model in AD research, the Stat6VT transgenic, constitutively expresses a mutant Stat6 that triggers downstream Th2 gene transcription without a stimulus in T and B cells.[13,14,33-36] Chronically activated Th2 cytokines drive the decrease in loricrin in keratinocytes, which over time manifests as lesions that resemble human AD.[13,14] Remarkably, no one has examined the oral cavity of these mice.

Few studies have investigated barrier dysfunction as a mechanism in periodontitis and SvP, and there is no animal model that mimics SvP.[17] Dermatologic studies have shown that CE protein expression alone does not always correlate with disease. Mislocalisation within the specific layers and within the cell can also alter barrier function.[5]

Our study aims to investigate the localisation and expression of CE proteins in human SvP gingival samples and compare to healthy controls. There is currently limited information as to the histologic presentation of these patients. Similarly, we will investigate CE proteins in Pg-infected and uninfected Stat6VT mice, a barrier-defect model, and compare with the human findings.

Methods

Methods are shown diagrammatically in Figures 1C (human) and 1D (mouse). Reagents were from Fisher Scientific unless otherwise indicated.

Human samples

Gingival discard samples, from areas without inflammation, were collected from 5 patients each with gingival health and IIIC and IVC disease at the University of Alberta Periodontology Clinic following informed consent (Pro00062112). Patients were diagnosed by a second- or third-year periodontology resident and confirmed by an instructor. There were 8 males and 7 females, aged 47 to 82 years. All patients were systemically healthy nonsmokers who were not taking any medications.

Mice and Mouse Samples

Stat6VT sperm were provided by Mark H. Kaplan (Indiana School of Medicine) for rederivation by the Jackson Laboratory. Stat6VT hemizygous mice were mated with C57Bl/6j mice to yield Stat6VT hemizygotes and littermate controls. All procedures were approved by the Animal Care and Use Committee of the University of Alberta (AUP 00002935). Mice were genotyped as previously described.[35,37,38]

Using a power calculation, in which a 25% difference in alveolar bone loss was considered significant, at 80% power, 9 mice per group were sufficient; 2 extra mice were included per group in case of unexpected morbidities/mortalities. Eleven mice per group were orally infected with Pg (ATCC strain #33277) by lavage under anaesthesia, as previously described.[39-41] For Ki67, CD45 and CK1 (mouse) cell counts, a sample size calculation showed that $n < 5$ gave 80% power with $P < .05$; we included 5 per group.

Mouse masticatory mucosa, from the incisive papilla to the soft palate, and mandibles were collected and preserved in 4% formaldehyde at 4 °C for 24 hours and then stored in phosphate-buffered saline (PBS).

Histology

Mouse mandibles were separated sagittally and decalcified in 0.5 M ethylenediaminetetraacetic acid, disodium salt dihydrate, pH 7.4 on a rotating platform; the solution was changed every other day for 8 weeks.[42]

Two- to five-mm tissue samples were immersed in 50% ethanol for 2 hours before automated processing (Leica

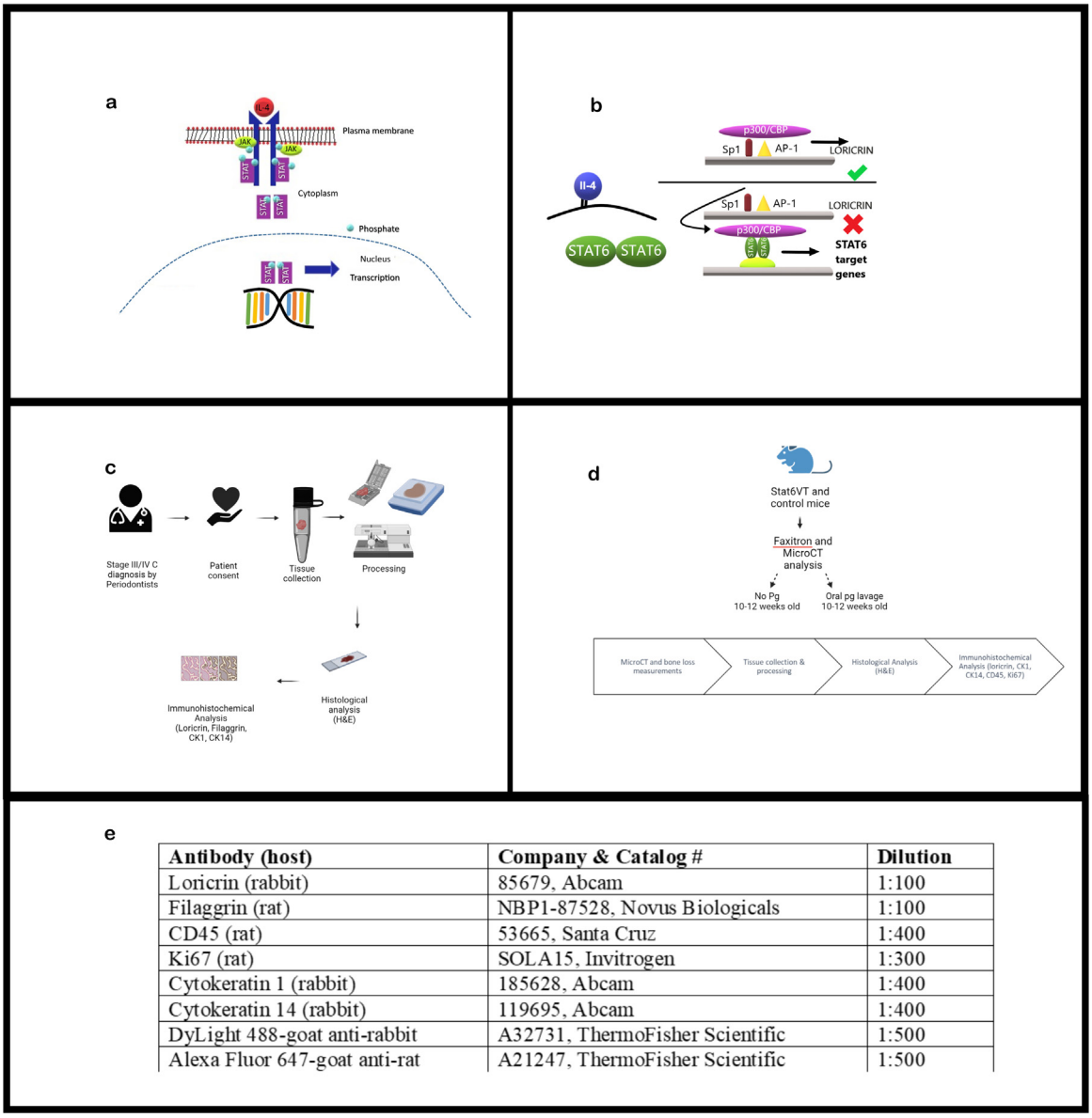

e

Antibody (host)	Company & Catalog #	Dilution
Loricrin (rabbit)	85679, Abcam	1:100
Filaggrin (rat)	NBP1-87528, Novus Biologicals	1:100
CD45 (rat)	53665, Santa Cruz	1:400
Ki67 (rat)	SOLA15, Invitrogen	1:300
Cytokeratin 1 (rabbit)	185628, Abcam	1:400
Cytokeratin 14 (rabbit)	119695, Abcam	1:400
DyLight 488-goat anti-rabbit	A32731, ThermoFisher Scientific	1:500
Alexa Fluor 647-goat anti-rat	A21247, ThermoFisher Scientific	1:500

Fig. 1 – A, Diagram of Jak-Stat pathway. B, During chronic interleukin (IL)-4 release, signal transducer and activator of transcription 6 (Stat6) uses p300/CREB-binding protein which is also needed for loricrin transcription. Methodological outline for (C) human and (D) mouse samples. E, Details for antibodies used in this study. Figures 1C and 1D were created with BioRender.com.

Biosystems, TP10). Samples were embedded (EG1160, Leica Biosystems) in Histoplast paraffin and sectioned (7 μm) using an automated microtome (RM2255, Leica). For human tissues, the histologic process was similar, except decalcification was unnecessary and CD45 and Ki67 immunostaining were not performed.

Hematoxylin and eosin (H&E) staining

Tissues were heated at 65 °C for 10 minutes to deparaffinise, and samples were rehydrated using xylene, graded ethanol, and Milli-Q water. Slides were immersed in hematoxylin (245656, Protocol) for 4 minutes, washed in Milli-Q water, and placed in eosin (245658, Protocol) for 30 seconds.[43] Sections were subsequently dehydrated in graded ethanol and xylene and mounted (Permount).

Immunofluorescence

Sections were deparaffinised, immersed in a boiling antigen retrieval solution (0.6 mM citric acid, 10 mM trisodium citrate buffer, pH 6.0) for 1.5 minutes and cooled for 40 minutes. After blocking with 10% goat serum (ab7481, Abcam) in tris-buffered saline for 45 minutes, sections were incubated with primary antibody in 1% bovine serum albumin overnight at 4 °C. Slides were washed 3 times in PBS + 1% Tween-20 for 5

minutes each and then incubated with secondary antibody for 1 hour. Details for antibodies are shown in Figure 1E. After washing as previously, sections were mounted utilising SlowFade Gold Antifade Mountant with DAPI.[44] Cell counts were performed for CD45, CK1 (mouse), and Ki67 by 3 calibrated and blinded examiners. Under 40× magnification, 3 random fields of the masticatory gingiva per mouse were assessed. For loricrin, filaggrin, CK1 (human), and CK14, descriptive and semiquantitative analyses only are provided.

Alveolar bone measurements

Before decalcification, fixed mouse heads were scanned using 3-dimensional micro-computerised tomography (Milabs U-SPECT-II/CT, 25 μm voxel size 70 kVp, 114 μA, 0.5 mm AL filter, 500 ms integration time). To measure alveolar bone levels, Avizo Software (version 9.1) and landmarks cementoenamel junction (CEJ), alveolar bone crest (ABC), and root apex (RA) of the left first and second mandibular molars were used.[45] Eight measurements were collected per tooth (sagittal plane: mesial and distal; coronal plane: distal, middle, and mesial lingual and buccal) by 3 blinded examiners calibrated according to Cohen's kappa inter/intra-reliability test (average acceptable error $\leq$ 3% or 0.2 mm).

Cytokine array

Relative levels of 96 cytokines were compared in 5 pooled plasma samples from control and Stat6VT mice using a mouse cytokine array (ab193659, Abcam). Incubation, washes, and signal development were as per the manufacturer. Pixel densities for the grid-identified duplicate spots for each cytokine were quantified using a ChemiDoc (XRS+, ImageLab, v 6.1.0, BioRad).

Statistical analyses

To determine normality, Shapiro–Wilk test was used, followed by Student *t* test for normally distributed data and Mann–Whitney *U* test if the values were not normally distributed. Significance was set at $P < .05$.

Results

Comparison of CE proteins in patients with SvP and healthy controls

Based on comparative fluorescent intensity to healthy controls, tissues from IIIC and IVC patients presented with decreased loricrin expression (Figure 2A–C). The protein was found in unexpected locations, such as spinous or basal layers. Filaggrin, largely contained to the upper layers of the epithelium in healthy and IIIC patients, became broadly expressed at low levels throughout the epithelium of IVC patients (Figure 2D–F). There was a slight but progressive increase in the distribution of CK1 in IIIC and IVC samples, accompanied by a decrease in expression (Figure 2G, 2H), which was more pronounced in IVC patients (Figure 2i). CK14 was broadly distributed in all layers in IIIC and IVC patients compared to controls (Figure 2J–L) and had the greatest expression in IIIC. H&E staining showed an increase in clear cells in IIIC and IVC patients (Figure 2M–O). Whilst the keratinised layer was of similar thickness in healthy tissues and those with disease, the spinous layer appeared broader in IIIC and IVC.

Characterisation of Stat6VT mice prior to Pg infection

Stat6VT male mice experienced skin lesions at 10 to 12 weeks of age; females had earlier and more variable disease onset (data not shown). Faxitron analysis of femurs showed no differences in bone mineral content/density for males at this age (Figure 3A–D); females showed significant differences. CEJ to ABC distance was significantly greater at 1 site on the first molar and 4 sites on the second molar in Stat6VT male mice compared with controls (Figure 3E–J). Neither sex showed any gross signs of oral inflammation. H&E staining of the masticatory mucosa revealed an increase in rete pegs and clear cells in male Stat6VT mice. This was confirmed with the pan leukocyte marker, CD45 (Stat6VT: 19.08 ± 0.7432 vs control: 11.08 ± 1.654 CD45+ cells/40× field, $P = .0012$). There was also significantly more proliferation in the epithelium of Stat6VT male mice (Stat6VT: 43.86 ± 3.42 vs control: 29.57 ± 3.416 Ki67+ cells/40× field, $P = .0039$). CK1 and CK14 expression were largely similar between the groups (Figure 3K–N). Loricrin expression was equal in intensity, but not confined to the granular layer in Stat6VT mice (Figure 3O and 3P).

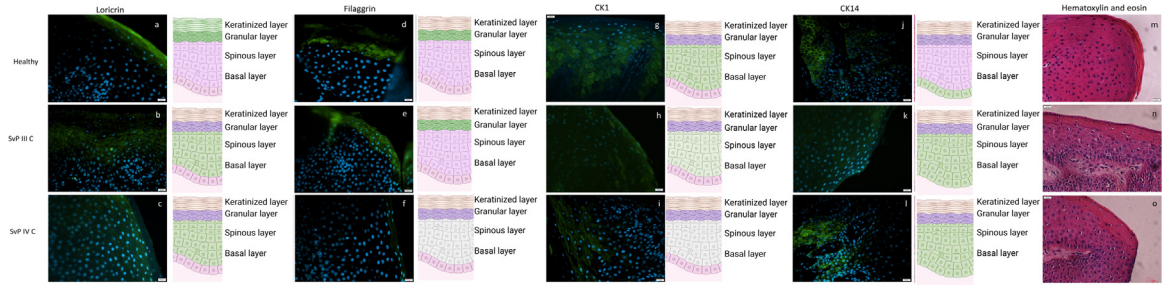

Fig. 2 – Gingival samples of healthy patients and those with severe periodontitis (SvP) immunostained with antibodies for loricrin (A–C), filaggrin (D–F), cytokeratin (CK)1 (G–I), CK14 (J–L), and hematoxylin and eosin (H&E) staining (M–O). n = 5/group, scale bar 20 μm.

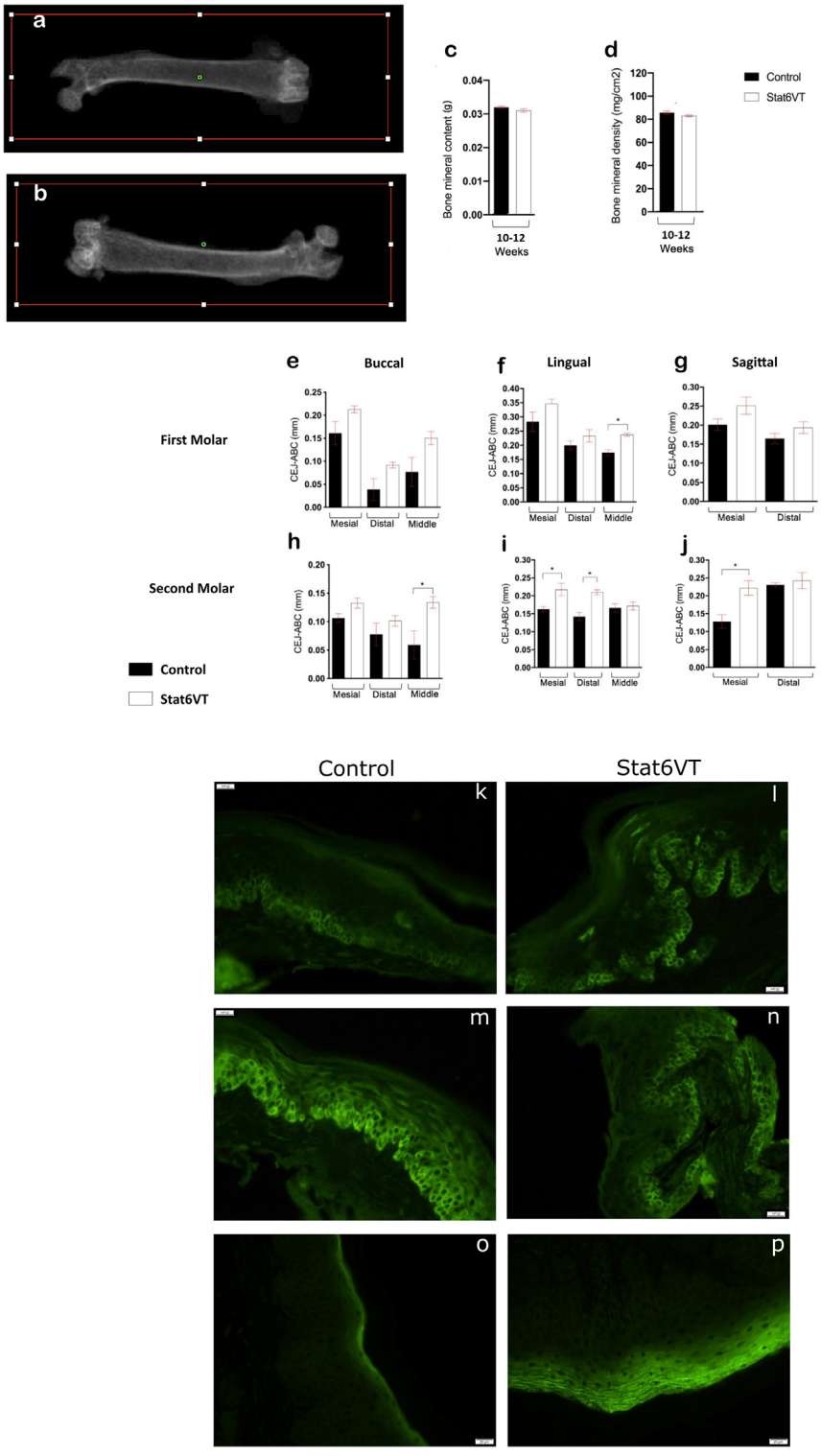

Fig. 3 – Bone mineral content and bone mineral density. Representative femurs from 12-week-old male mice. A, Control femur (bone mineral content [BMC]: 0.03230 g; bone mineral density [BMD]: 80.945 mg/cm^2). B, Signal transducer and activator of transcription 6 (Stat6VT) femur (BMC: 0.03064 g; BMD: 80.848 mg/cm^2). Quantification of femur BMC (C) and BMD (D) of control and Stat6VT 12-week-old male mice (n = 5/group). Micro-computerised tomography measurements of molars from 12-week-old male Stat6VT and control mice with no Pg infection (n = 5/group): E, first molar buccal aspect; F, first molar lingual aspect; G, first molar sagittal aspect; H, second molar buccal aspect; I, second molar lingual aspect; J, second molar sagittal aspect. CK1 positive cells in the masticatory mucosa of 12-week-old male mice with no *Porphyromonas gingivalis* (Pg) infection (n = 5/group): K, control; L, Stat6VT mice. CK14 positive cells in the masticatory mucosa of 12-week-old male mice with no Pg infection (n = 5/group): M, control; N, Stat6VT mice. Loricrin staining in the masticatory mucosa of 12-week-old male mice with no Pg infection (n = 5/group): O, control; P, Stat6VT mice. Scale bar 20 μm.

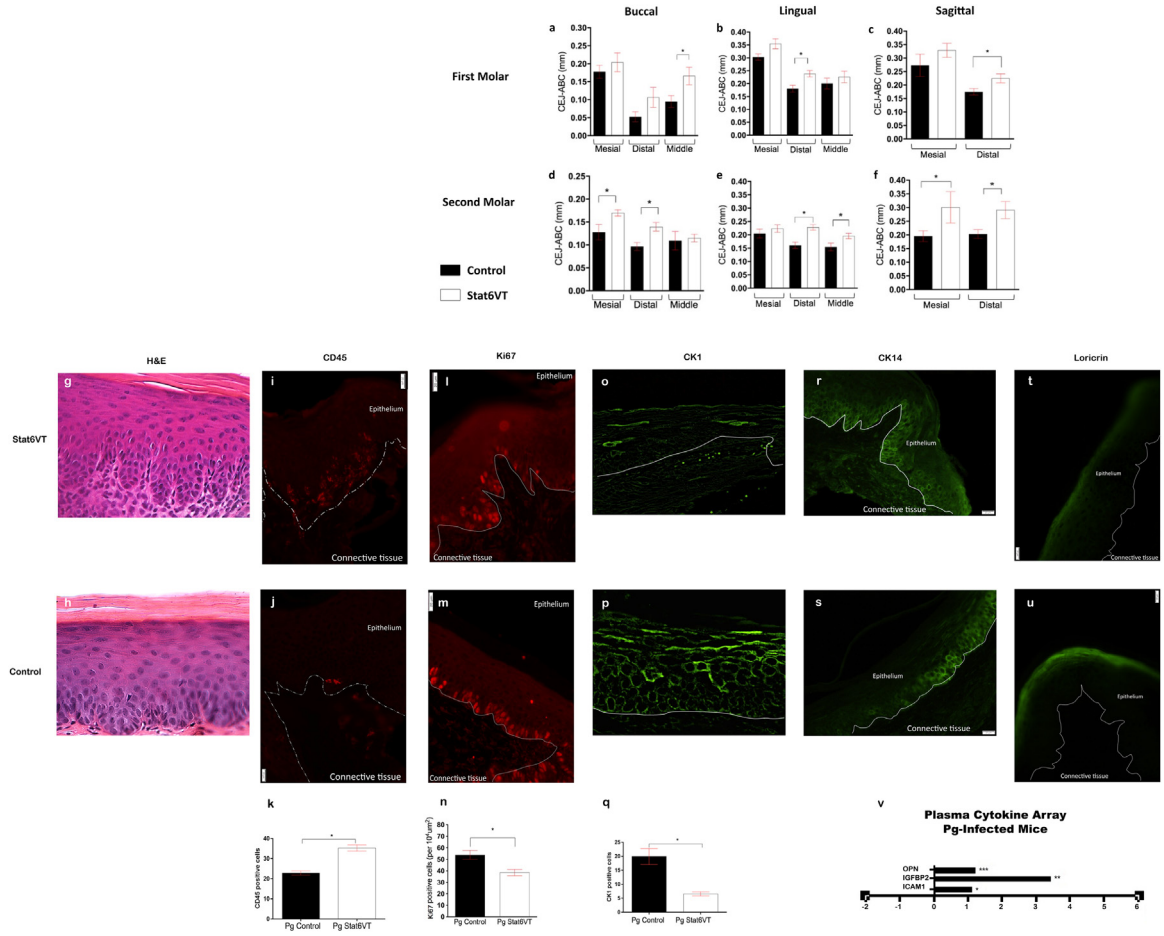

Fig. 4 – Micro-computerised tomography measurements of molars from 12-week-old male *Porphyromonas gingivalis* (Pg) –infected signal transducer and activator of transcription 6 (Stat6VT) and control mice (n = 5/group): A, first molar buccal aspect; B, first molar lingual aspect; C, first molar sagittal aspect; D, second molar buccal aspect; E, second molar lingual aspect; F, second molar sagittal aspect. Hematoxylin and eosin (H&E) staining of masticatory mucosa from Pg-infected male mice (n = 5/group): G, control; H, Stat6VT. CD45 positive cells in the masticatory mucosa from Pg-infected male mice (n = 5/group): I, control; J, Stat6VT mice; quantification is shown in (K). The white dashed line demarcates the basal layer of the epithelium for reference. CK1 positive cells in the masticatory mucosa from Pg-infected male mice (n = 5/group): L, control; M, Stat6VT mice; quantification is shown in (N). The white line demarcates the basal layer of the epithelium for reference. Ki67 positive cells in the masticatory mucosa from Pg-infected male mice (n = 5/group): O, control; P, Stat6VT mice; quantification is shown in (Q). The white line demarcates the basal layer of the epithelium for reference. CK14 positive cells in the masticatory mucosa from Pg-infected male mice (n = 5/group): R, control; S, Stat6VT mice. The white line demarcates the basal layer of the epithelium for reference. Loricrin staining in the masticatory mucosa of Pg-infected male mice (n =5/group): T, control; U, Stat6VT mice. The white line demarcates the basal layer of the epithelium for reference. Scale bar 20 μm. V, Plasma cytokine array results expressed as fold change Pg-infected male Stat6VT mice/control (n = 5 pooled samples/group).

Pg-infected Stat6VT mice have more severe effects

We chose 10- to 12-week-old males for the PD study because skin disease onset and progression were more uniform and bone mineral density/content did not differ from controls. Pg is a keystone pathogen that creates a biofilm dysbiosis, leading to inflammation and bone loss consistent with PD.[46-49] The CEJ to ABC distance was significantly greater in 9 of 16 assessed sites in Pg-infected Stat6VT compared to Pg-infected control mice. Three sites were located on the first molar (Figure 4A–C) and six on the second molar (Figure 4D–F).

H&E staining of the masticatory mucosa was again suggestive of increased inflammation in Pg-infected Stat6VT mice compared with controls; there were more clear cells and rete pegs (Figure 4G and 4H), and more patches of cells clustered around the basal layer and across the spinous layer, suggestive of an inflammatory infiltrate. These findings were confirmed by CD45 cell counts (Figure 4I–K).

As observed in Pg-infected controls, Ki67 usually is expressed exclusively in the basal layer. In Pg-infected Stat6VT mice, clusters of Ki67+ cells traveled up the rete pegs (Figure 4L and 4M). There was a greater number of

Table – Comparison of assessed parameters amongst the groups.

	Healthy human control	SvP IIIC	SvP IVC	Control mice	Stat6VT mice	Control mice + Pg	Stat6VT mice + Pg
H&E	*Normal architecture; no signs of inflammation*	*Increase in clear cells; broader spinous layer*	*Increase in clear cells; broader spinous layer*	*Normal architecture; no signs of inflammation*	*Increased rete pegs and clear cells*	*Increased rete pegs and clear cells*	*Increased rete pegs and clear cells vs control + Pg; inflammatory infiltrate*
Loricrin	*Signal of bright intensity restricted to keratinised and granular layer*	*Decrease in signal intensity; signal spreads to lower layers*	*Decrease in signal intensity; signal spreads to lower layers*	*Signal of bright intensity restricted to keratinised and granular layer*	*Signal of bright intensity; signal spreads to lower layers*	*Signal of bright intensity restricted to keratinised and granular layer*	*Decrease in signal intensity; signal spreads to lower layers*
Filaggrin	*Signal of bright intensity restricted to keratinised and granular layer*	*Signal of bright intensity restricted to keratinised and granular layer*	*Decrease in signal intensity*	*N/A*	*N/A*	*N/A*	*N/A*
CK1	*Signal of bright intensity restricted to spinous and granular layer*	*Decrease in signal intensity*	*Decrease in signal intensity*	*Signal of bright intensity restricted to spinous and granular layer*	*Increased signal intensity on the basal layers*	*Signal of bright intensity restricted to spinous and granular layer*	*Decrease in signal intensity*
CK14	*Signal of bright intensity restricted to basal and suprabasal cells*	*Similar signal intensity; signal spreads above basal layer*	*Similar signal intensity; signal spreads above basal layer*	*Signal of bright intensity restricted to basal and suprabasal cells*	*Similar signal intensity; signal spreads above basal layer*	*Signal of bright intensity restricted to basal and suprabasal cells*	*Similar signal intensity; signal spreads above basal layer*
CD45	*N/A*	*N/A*	*N/A*	*11.08 ± 1.654*	*19.08 ± 0.7432*[*]	*22.86 ± 1.067*	*35.30 ± 1.539*[#]
Ki67	*N/A*	*N/A*	*N/A*	*29.57 ± 3.416*	*43.86 ± 3.42*[*]	*53.97 ± 3.870*	*38.54 ± 2.637*[#]

CK, cytokeratin; H&E, hematoxylin and eosin staining; N/A, not assessed; Pg, *Porphyromonas gingivalis*; Stat6VT, signal transducer and activator of transcription 6; SvP, severe periodontitis

[*] $P < .05$ when compared with control group.
[#] $P < .05$ when compared with control mice + Pg.

Ki67+ cells in Pg-infected control vs Pg-infected Stat6VT mice (Figure 4N).

CK1 expression showed dramatic decrease in Pg-infected Stat6VT mice (Figure 4O–Q). CK14, in contrast, was more broadly expressed, extending from the basal layer into the granular layer (Figure 4R and 4S). Loricrin was not confined to the keratinised and granular layer, and immunofluorescent intensity was decreased in Pg-infected Stat6VT mice (Figure 4T and 4U). These data suggested an overall disruption of the tightly regulated CE differentiation pathway. Tabulation of results for comparison is found in the Table.

Of the 96 cytokines measured, there was ≥1-fold increase in expression of osteopontin (OPN), intercellular adhesion molecule (ICAM) 1, and insulin-like growth factor binding protein (IGFBP) 2 in Stat6VT mice (Figure 4V); there were many cytokines similarly expressed in both groups.

Discussion

We employed a unique mouse model for our studies, the Stat6VT transgenic, which is extensively used in AD research. Recent studies implicate a role for the Th2 cytokine IL-4 in SvP and show that Pg can affect CE protein expression via this mechanism.[13,50-60] We hypothesised that in the condition of reduced barrier function, the effects of Pg infection would be exaggerated. Using the most common human isolate of Pg, ATCC 33277, our results revealed enhanced bone loss and inflammation as well as dysregulation of CE and CK proteins, suggesting disruption of the normal differentiation process. We compared histologic findings in the mouse model to human SvP. Because PD is primarily a clinical diagnosis, little has been published regarding SvP histologic presentation. In addition to noting decreased/disorganised loricrin expression, we found similarities in the change in expression of cytokeratins. A hypothesis for future study is whether patients with SvP have already reduced barrier function that is then worsened by Pg infection, leading to greater disease.

Pg-infected Stat6VT mice demonstrated a greater reduction in alveolar bone levels compared with controls. These findings align with our hypothesis, as we expected an augmented inflammatory response to the pathogenic bacteria, with a greater effect due to altered barrier integrity in Stat6VT mice. Oral tissues from Pg-infected Stat6VT mice showed an inflammatory response above what was noted in controls and uninfected Stat6VT mice.[61] These findings mirror what was observed in patients with SvP.[62,63]

Cytokeratins provide epithelial mechanical support, maintain cell architecture, and are important in intercellular transport, nuclear integrity, and protein synthesis.[8] They connect with desmosomes and hemidesmosomes to form tight junctions between cells, the extracellular matrix, and

surrounding cells. Junction defects contribute to skin and bowel diseases and increase systemic exposure to bacterial lipopolysaccharide.[64]

CK1 is typically observed in suprabasal layers of the keratinised oral epithelium and skin.[8,65-67] In pathogen-challenged Stat6VT oral epithelium and patients with SvP, CK1 immunofluorescence signal was decreased compared with controls. CK1 expression normally increases during cell turnover and healing processes, since it is involved in epithelial barrier maintenance, repair, DNA processing, cell proliferation, and differentiation.[7,68,69] Studies show CK1 dysregulation in inflammatory and proliferative diseases.[7,69] Downregulation of CK1 has been observed in induced human gingivitis after 21 days and may be considered a marker of chronic epithelial stress.[70] Given that periodontal disease is a spectrum disorder, we consider that this downregulation would progress with disease progression, but this would need future study for confirmation.

CK14 is a marker of proliferating cells; once cells enter into the differentiation programme, CK14 is silenced.[71,72] Expanded expression of CK14 to suprabasal layers is observed in chronic wound healing or poorly differentiated carcinomas.[73] Mislocalisation of CK14 could be a marker of a stressed and inflamed oral epithelium and also suggests less terminal differentiation.[68,69,73] The loss of CK1:CK10 in suprabasal layers as a result of replacement by CK14 may disrupt the differentiation process, reduce epithelial strength and, consequently, impair barrier integrity.[74] Increased CK14 expression has been associated with greater epithelial fragility.[75]

After Pg infection, loricrin expression was weaker and distributed beyond the uppermost layers in Stat6VT mice compared with controls. In healthy human oral epithelium, loricrin showed confined expression to the upper layers; in contrast, there was a profound decrease in immunofluorescent signal intensity in all patients with SvP and a broader distribution. Further study is necessary to understand whether the wider distribution of loricrin in nonkeratinised layers of the oral epithelium has functional consequences.

The appearance of Ki67 in suprabasal layers has been related to oral epithelial dysplasia.[76,77] This finding in Pg-infected Stat6VT mice aligns with the deranged CE protein distribution and expression.[77] In Pg-infected Stat6VT mice, the number of Ki67+ cells was reduced (opposite to what was observed in the uninfected mice). This again suggests greater chronic inflammation in these mice.[76,77]

Many cytokines were similarly expressed in Stat6VT and control mice infected with Pg, but those that were increased above levels in control mice were quite compelling considering their function and relationship to PD. IGFBP-2 plays a significant role in bone metabolism.[78] It rises with age and is a strong predictor of decreasing bone mineral density.[79-81] Consistent with our findings, IGFBP-2 expression was observed to be induced by Pg, and studies in humans have shown that greater concentrations of IGFBP-2 correlate with increased probing depth and may be an indicator of PD progression.[82,83] OPN, also known as bone sialoprotein 1, is essential for bone remodelling and biomineralisation during stress.[84] OPN increases in periodontitis and is related to increased proliferation and differentiation of osteoclasts.[84-88] ICAM-1 has been implicated in a variety of chronic systemic immune and inflammatory responses and is overexpressed in inflamed gingival tissues.[89] Expression of ICAM-1, an adhesion receptor, on human microvascular endothelial cells has been shown to facilitate Pg invasion.[89-93] Increased invasion would enhance speed of disease progression, as observed in Stat6VT mice and SvP.[94,95]

Past studies have categorised patients as having aggressive or chronic periodontitis. Not all patients with SvP would be considered in the aggressive category. This is a limitation of our interpretation of these studies with past research. A major difference between aggressive periodontitis patients and IIIC and IVC patients is age and disease modifiers. To be consistent with previous studies, only patients who were systemically healthy and nonsmokers were included in this study.

Our assessment of CE proteins was qualitative and semiquantitative, which is a limitation. Immunohistochemistry allows one to distinguish nonkeratinised from keratinised tissue and to visualise localisation of proteins. However, this method is less quantitative compared with western blot or enzyme-linked immunosorbent assay.

A limitation of the Stat6VT model is overexpression of Stat6. This may be potentially confounding, as it is an important factor for lymphocyte proliferation, gene expression (eg, IL-4 induced genes), and T-cell differentiation.[38] We chose age and sex such that there were few differences from controls to minimise potential confounding.

Conflict of interest

None disclosed.

Acknowledgements

We thank Dr Pranidhi Baddam for assistance in micro-computerised tomography scanning of mice heads and Dr Manuel Lagravere Vich for his assistance in creating the micro-computerised tomography protocol.

Funding

This work was funded by Canadian Institutes of Health and Research, University Hospital Foundation, The Fund for Dentistry, and the Dental Hygiene Graduate Student Research Fund.

REFERENCES

1. Candi E, Schmidt R, Melino G. The cornified envelope: a model of cell death in the skin. Nat Rev Mol Cell Biol 2005;6(4):328–40.
2. Darlenski R KJ, Tsankov N. Skin barrier function: morphological basis and regulatory mechanisms. J Clin Med 2011;4:36–45.
3. Menon GK, Cleary GW, Lane ME. The structure and function of the stratum corneum. Int J Pharm 2012;435(1):3–9.
4. Nemes Z, Steinert PM. Bricks and mortar of the epidermal barrier. Exp Mol Med 1999;31(1):5–19.

5. Catunda R, Rekhi U, Clark D, Levin L, Febbraio M. Loricrin downregulation and epithelial-related disorders: a systematic review. J Dtsch Dermatol Ges 2019;17(12):1227–38.
6. Nithya S, Radhika T, Jeddy N. Loricrin - an overview. J Oral Maxillofac Pathol 2015;19(1):64–8.
7. Dong X, Liu Z, Lan D, et al. Critical role of Keratin 1 in maintaining epithelial barrier and correlation of its down-regulation with the progression of inflammatory bowel disease. Gene 2017;608:13–9.
8. Rao RS, Patil S, Ganavi BS. Oral cytokeratins in health and disease. J Contemp Dent Pract 2014;15(1):127–36.
9. Ishida-Yamamoto A, Takahashi H, Iizuka H. Loricrin and human skin diseases: molecular basis of loricrin keratodermas. Histol Histopathol 1998;13(3):819–26.
10. O'Regan GM, Sandilands A, McLean WHI. Irvine AD. Filaggrin in atopic dermatitis. J Allergy Clin Immunol 2008;122(4):689–93.
11. Schmuth M, Fluhr JW, Crumrine DC, et al. Structural and functional consequences of loricrin mutations in human loricrin keratoderma (Vohwinkel syndrome with ichthyosis). J Invest Dermatol 2004;122(4):909–22.
12. Bussmann C, Weidinger S, Novak N. Genetics of atopic dermatitis. J Dtsch Dermatol Ges 2011;9(9):670–6.
13. Bao L, Mohan GC, Alexander JB, et al. A molecular mechanism for IL-4 suppression of loricrin transcription in epidermal keratinocytes: implication for atopic dermatitis pathogenesis. Innate Immun 2017;23(8):641–7.
14. Kim BE, Leung DY, Boguniewicz M, Howell MD. Loricrin and involucrin expression is down-regulated by Th2 cytokines through STAT-6. Clin Immunol 2008;126(3):332–7.
15. Goenka S, Kaplan MH. Transcriptional regulation by STAT6. Immunol Res 2011;50(1):87–96.
16. Yamada M, Takahashi N, Matsuda Y, et al. A bacterial metabolite ameliorates periodontal pathogen-induced gingival epithelial barrier disruption via GPR40 signaling. Sci Rep 2018;8(1):9008.
17. Caetano AJ, Yianni V, Volponi A, Booth V, D'Agostino EM, Sharpe P. Defining human mesenchymal and epithelial heterogeneity in response to oral inflammatory disease. eLife 2021;10:e62810.
18. Katz J, Sambandam V, Wu JH, Michalek SM, Balkovetz DF. Characterization of *Porphyromonas gingivalis*-induced degradation of epithelial cell junctional complexes. Infect Immun 2000;68(3):1441–9.
19. Lagha AB, Groeger S, Meyle J, Grenier D. Green tea polyphenols enhance gingival keratinocyte integrity and protect against invasion by Porphyromonas gingivalis. Pathog Dis 2018;76(4).
20. Katz J, Yang Q-B, Zhang P, Potempa J, Travis J, Michalek SM, et al. Hydrolysis of Epithelial Junctional Proteins by Porphyromonas gingivalis Gingipains. Infect Immun 2002;70(5):2512–8.
21. Abe-Yutori M, Chikazawa T, Shibasaki K, Murakami S. Decreased expression of E-cadherin by Porphyromonas gingivalis-lipopolysaccharide attenuates epithelial barrier function. J Periodontal Res 2017;52(1):42–50.
22. Guo W, Wang P, Liu Z-H, Ye P. Analysis of differential expression of tight junction proteins in cultured oral epithelial cells altered by *Porphyromonas gingivalis*, *Porphyromonas gingivalis* lipopolysaccharide, and extracellular adenosine triphosphate. Int J Oral Sci 2018;10(1) e8–e.
23. Nakagawa I, Amano A, Inaba H, Kawai S, Hamada S. Inhibitory effects of *Porphyromonas gingivalis* fimbriae on interactions between extracellular matrix proteins and cellular integrins. Microbes Infect 2005;7(2):157–63.
24. Amano A. Disruption of epithelial barrier and impairment of cellular function by Porphyromonas gingivalis. Front Biosci 2007;12:3965–74.
25. Kalinin AE, Kajava AV, Steinert PM. Epithelial barrier function: assembly and structural features of the cornified cell envelope. Bioessays 2002;24(9):789–800.
26. Caton JG, Armitage G, Berglundh T, et al. A new classification scheme for periodontal and peri-implant diseases and conditions - introduction and key changes from the 1999 classification. J Periodontol 2018;89(Suppl 1):S1–8.
27. Nowak M, Kramer B, Haupt M, et al. Activation of invariant NK T cells in periodontitis lesions. J Immunol 2013;190(5):2282–91.
28. Guzeldemir-Akcakanat E, Sunnetci-Akkoyunlu D, Orucguney B, et al. Gene-expression profiles in generalized aggressive periodontitis: a gene network-based microarray analysis. J Periodontol 2016;87(1):58–65.
29. Suzuki A, Horie T, Numabe Y. Investigation of molecular biomarker candidates for diagnosis and prognosis of chronic periodontitis by bioinformatics analysis of pooled microarray gene expression datasets in Gene Expression Omnibus (GEO). BMC Oral Health 2019;19(1):52.
30. Sharma A, Raman A, Pradeep AR. Association of chronic periodontitis and psoriasis: periodontal status with severity of psoriasis. Oral Dis 2015;21(3):314–9.
31. Bartova J, Kratka-Opatrna Z, Prochazkova J, et al. Th1 and Th2 cytokine profile in patients with early onset periodontitis and their healthy siblings. Mediators Inflamm 2000;9(2):115–20.
32. Reichle ME, Chen L, Lin SX, Chan LS. The Th2 systemic immune milieu enhances cutaneous inflammation in the K14-IL-4-transgenic atopic dermatitis model. J Invest Dermatol 2011;131(3):791–4.
33. Sehra S, Krishnamurthy P, Koh B, et al. Increased Th2 activity and diminished skin barrier function cooperate in allergic skin inflammation. Eur J Immunol 2016;46(11):2609–13.
34. Sehra S, Bruns HA, Ahyi AN, et al. IL-4 is a critical determinant in the generation of allergic inflammation initiated by a constitutively active Stat6. J Immunol 2008;180(5):3551–9.
35. DaSilva-Arnold SC, Thyagarajan A, Seymour LJ, et al. Phenotyping acute and chronic atopic dermatitis-like lesions in Stat6VT mice identifies a role for IL-33 in disease pathogenesis. Arch Dermatol Res 2018;310(3):197–207.
36. Turner MJ, DaSilva-Arnold S, Luo N, et al. STAT6-mediated keratitis and blepharitis: a novel murine model of ocular atopic dermatitis. Investig Ophthalmol Vis Sci 2014;55(6):3803–8.
37. Bruns HA, Schindler U, Kaplan MH. Expression of a constitutively active Stat6 in vivo alters lymphocyte homeostasis with distinct effects in T and B cells. J Immunol 2003;170(7):3478–87.
38. Kaplan MH, Sehra S, Chang HC, O'Malley JT, Mathur AN, Bruns HA. Constitutively active STAT6 predisposes toward a lymphoproliferative disorder. Blood 2007;110(13):4367–9.
39. Rekhi UR, Catunda RQ, Alexiou M, Sharma M, Fong A, Febbraio M. Impact of a CD36 inhibitor on *Porphyromonas gingivalis* mediated atherosclerosis. Arch Oral Biol 2021;126:105129.
40. Lalla E, Lamster IB, Hofmann MA, et al. Oral infection with a periodontal pathogen accelerates early atherosclerosis in apolipoprotein E-null mice. Arterioscler Thromb Vasc Biol 2003;23(8):1405–11.
41. Brown PM, Kennedy DJ, Morton RE, Febbraio M. CD36/SR-B2-TLR2 dependent pathways enhance *Porphyromonas gingivalis* mediated atherosclerosis in the Ldlr KO mouse model. PLoS One 2015;10(5):e0125126.
42. Berlin-Broner Y, Alexiou M, Levin L, Febbraio M. Characterization of a mouse model to study the relationship between apical periodontitis and atherosclerosis. Int Endod J 2020;53(6):812–23.
43. Slaoui M, Bauchet AL, Fiette L. Tissue sampling and processing for histopathology evaluation. Methods Mol Biol 2017;1641:101–14.

44. Kim MJ, Kim JY, Kang M, Won MH, Hong SH. Her Y. Reduced fecal calprotectin and inflammation in a murine model of atopic dermatitis following probiotic treatment. Int J Mol Sci 2020;21(11):3968.
45. Catunda RQ, Ho KK-Y, Patel S, Febbraio M. A 2-plane micro-computed tomographic alveolar bone measurement approach in mice. Imaging Sci Dent 2021;51(4):389–98.
46. How KY, Song KP, Chan KG. *Porphyromonas gingivalis*: an overview of periodontopathic pathogen below the gum line. Front Microbiol 2016;7:53.
47. Gully N, Bright R, Marino V, et al. *Porphyromonas gingivalis* peptidylarginine deiminase, a key contributor in the pathogenesis of experimental periodontal disease and experimental arthritis. PLoS One 2014;9(6):e100838.
48. Xu W, Zhou W, Wang H, Liang S. Roles of *Porphyromonas gingivalis* and its virulence factors in periodontitis. Adv Protein Chem Struct Biol 2020;120:45–84.
49. Wilensky A, Gabet Y, Yumoto H, Houri-Haddad Y, Shapira L. Three-dimensional quantification of alveolar bone loss in *Porphyromonas gingivalis*-infected mice using micro-computed tomography. J Periodontol 2005;76(8):1282–6.
50. Gonzales JR, Mann M, Stelzig J, Bodeker RH, Meyle J. Single-nucleotide polymorphisms in the IL-4 and IL-13 promoter region in aggressive periodontitis. J Clin Periodontol 2007;34 (6):473–9.
51. Gonzales JR, Groger S, Haley G, Bodeker RH, Meyle J. The interleukin-4 -34TT and -590TT genotype is correlated with increased expression and protein production in aggressive periodontitis. Mol Immunol 2010;47(4):701–5.
52. Giardina E, Capon F, De Rosa MC, et al. Characterization of the loricrin (LOR) gene as a positional candidate for the PSORS4 psoriasis susceptibility locus. Ann Hum Genet 2004;68(Pt 6):639–45.
53. Sugiura H, Ebise H, Tazawa T, et al. Large-scale DNA microarray analysis of atopic skin lesions shows overexpression of an epidermal differentiation gene cluster in the alternative pathway and lack of protective gene expression in the cornified envelope. Br J Dermatol 2005;152(1):146–9.
54. Jarzab J, Filipowska B, Zebracka J, et al. Locus 1q21 Gene expression changes in atopic dermatitis skin lesions: deregulation of small proline-rich region 1A. Int Arch Allergy Immunol 2010;151(1):28–37.
55. Maestrini E, Monaco AP, McGrath JA, et al. A molecular defect in loricrin, the major component of the cornified cell envelope, underlies Vohwinkel's syndrome. Nat Genet 1996;13(1):70–7.
56. Song S, Shen C, Song G, et al. A novel c.545-546insG mutation in the loricrin gene correlates with a heterogeneous phenotype of loricrin keratoderma. Br J Dermatol 2008;159(3):714–9.
57. Yoneda K, Steinert PM. Overexpression of human loricrin in transgenic mice produces a normal phenotype. Proc Natl Acad Sci U S A 1993;90(22):10754–8.
58. Jarnik M, de Viragh PA, Scharer E, et al. Quasi-normal cornified cell envelopes in loricrin knockout mice imply the existence of a loricrin backup system. J Invest Dermatol 2002;118 (1):102–9.
59. Kim BE, Howell MD, Guttman-Yassky E, et al. TNF-alpha downregulates filaggrin and loricrin through c-Jun N-terminal kinase: role for TNF-alpha antagonists to improve skin barrier. J Invest Dermatol 2011;131(6):1272–9.
60. Suga Y, Jarnik M, Attar PS, et al. Transgenic mice expressing a mutant form of loricrin reveal the molecular basis of the skin diseases, Vohwinkel syndrome and progressive symmetric erythrokeratoderma. J Cell Biol 2000;151(2):401–12.
61. Nanci A, Ten Cate AR. Ten Cate's oral histology: development, structure, and function. 8th ed. St. Louis: Elsevier; 2013.
62. Nath SG, Raveendran R. "What is there in a name?": a literature review on chronic and aggressive periodontitis. J Indian Soc Periodontol 2011;15(4):318–22.
63. Catunda RQ, Levin L, Kornerup I, Gibson MP. Diagnosis of aggressive periodontitis: a dilemma? Quintessence Int 2018;49(3):173–80.
64. Candelli M, Franza L, Pignataro G, et al. Interaction between lipopolysaccharide and gut microbiota in inflammatory bowel diseases. Int J Mol Sci 2021;22(12):6242.
65. Garant PR. Oral cells and tissues. 1st ed. Chicago: Quintessence Pub. Co; 2003.
66. Dale BA, Salonen J, Jones AH. New approaches and concepts in the study of differentiation of oral epithelia. Crit Rev Oral Biol Med 1990;1(3):167–90.
67. Orban BJ, Bhaskar SN. Orban's oral histology and embryology. 11th ed. St. Louis: Mosby-Year Book; 1991.
68. Lauer G, Wiedmann-Al-Ahmad M, Otten JE, Hubner U. Immunohistochemical study during healing of free palatal mucosa grafts on plastic-embedded samples. J Oral Pathol Med 2001;30(2):104–12.
69. Knippschild U, Kruger M, Richter J, et al. The CK1 family: contribution to cellular stress response and its role in carcinogenesis. Front Oncol 2014;4:96.
70. Jonsson D, Ramberg P, Demmer RT, Kebschull M, Dahlen G, Papapanou PN. Gingival tissue transcriptomes in experimental gingivitis. J Clin Periodontol 2011;38(7):599–611.
71. Lane EB, McLean WH. Keratins and skin disorders. J Pathol 2004;204(4):355–66.
72. Omary MB, Coulombe PA, McLean WH. Intermediate filament proteins and their associated diseases. N Engl J Med 2004;351 (20):2087–100.
73. Sorlie T, Perou CM, Tibshirani R, et al. Gene expression patterns of breast carcinomas distinguish tumor subclasses with clinical implications. Proc Natl Acad Sci USA 2001;98 (19):10869–74.
74. Rivarola de Gutierrez E, Innocenti AC, Cippitelli MJ, Salomon S, Vargas-Roig LM. Determination of cytokeratins 1, 13 and 14 in oral lichen planus. Med Oral Patol Oral Cir Bucal 2014;19(4):e359–65.
75. Vassar R, Coulombe PA, Degenstein L, Albers K, Fuchs E. Mutant keratin expression in transgenic mice causes marked abnormalities resembling a human genetic skin disease. Cell 1991;64(2):365–80.
76. Takkem A, Barakat C, Zakaraia S, et al. Ki-67 prognostic value in different histological grades of oral epithelial dysplasia and oral squamous cell carcinoma. Asian Pac J Cancer Prev 2018;19(11):3279–86.
77. Birajdar SS, Radhika M, Paremala K, Sudhakara M, Soumya M, Gadivan M. Expression of Ki-67 in normal oral epithelium, leukoplakic oral epithelium and oral squamous cell carcinoma. J Oral Maxillofac Pathol 2014;18(2):169–76.
78. Beattie J, Al-Khafaji H, Noer PR, et al. Insulin-like growth factor-binding protein action in bone tissue: a key role for pregnancy- associated plasma protein-A. Front Endocrinol (Lausanne) 2018;9:31.
79. Xi G, Wai C, DeMambro V, Rosen CJ, Clemmons DR. IGFBP-2 directly stimulates osteoblast differentiation. J Bone Miner Res 2014;29(11):2427–38.
80. Allard JB, Duan C. IGF-binding proteins: why do they exist and why are there so many? Front Endocrinol (Lausanne) 2018;9:117.
81. Amin S, Riggs BL, Atkinson EJ, Oberg AL, Melton 3rd LJ, Khosla S. A potentially deleterious role of IGFBP-2 on bone density in aging men and women. J Bone Miner Res 2004;19(7):1075–83.
82. Zhou Q, Amar S. Identification of proteins differentially expressed in human monocytes exposed to *Porphyromonas gingivalis* and its purified components by high-throughput immunoblotting. Infect Immun 2006;74(2):1204–14.
83. Takenouchi Y, Ohshima M, Yamaguchi Y, et al. Insulin-like growth factor-binding protein-2 and -3 in gingival crevicular fluid. J Periodontal Res 2010;45(6):803–8.

84. Lund SA, Giachelli CM, Scatena M. The role of osteopontin in inflammatory processes. J Cell Commun Signal 2009; 3(3-4):311–22.
85. Buommino E, Tufano MA, Balato N, et al. Osteopontin: a new emerging role in psoriasis. Arch Dermatol Res 2009;301(6):397–404.
86. Dong M, Yu X, Chen W, et al. Osteopontin promotes bone destruction in periapical periodontitis by activating the NF-kappaB pathway. Cell Physiol Biochem 2018;49(3):884–98.
87. Parent RA. Comparative biology of the normal lung. 2nd ed. San Diego: Academic Press; 2015.
88. Singh A, Gill G, Kaur H, Amhmed M, Jakhu H. Role of osteopontin in bone remodeling and orthodontic tooth movement: a review. Prog Orthod 2018;19(1):18.
89. Chang LC, Kuo HC, Chang SF, et al. Regulation of ICAM-1 expression in gingival fibroblasts infected with high-glucose-treated *P. gingivalis*. Cell Microbiol 2013;15(10):1722–34.
90. Muller N. The role of intercellular adhesion molecule-1 in the pathogenesis of psychiatric disorders. Front Pharmacol 2019;10:1251.
91. Figenschau SL, Knutsen E, Urbarova I, et al. ICAM1 expression is induced by proinflammatory cytokines and associated with TLS formation in aggressive breast cancer subtypes. Sci Rep 2018;8(1):11720.
92. Gemmell E, Walsh LJ, Savage NW, Seymour GJ. Adhesion molecule expression in chronic inflammatory periodontal disease tissue. J Periodontal Res 1994;29(1):46–53.
93. Reyes L, Getachew H, Dunn WA. Progulske-Fox A. Porphyromonas gingivalis W83 traffics via ICAM1 in microvascular endothelial cells and alters capillary organization in vivo. J Oral Microbiol 2020;12(1):1742528.
94. Sun Q, Zhang Z, Ou Y. A allele of ICAM-1 Rs5498 and VCAM-1 Rs3181092 is correlated with increased risk for periodontal disease. Open Life Sci 2019;14:638–46.
95. Lima PM, Souza PE, Costa JE, Gomez RS, Gollob KJ, Dutra WO. Aggressive and chronic periodontitis correlate with distinct cellular sources of key immunoregulatory cytokines. J Periodontol 2011;82(1):86–95.